

Robust NIRS models for non-destructive prediction of physicochemical properties and ageing of basmati rice

Abstract:

Aim: To determine physicochemical properties and age of rice by non-destructive technique.

Place and duration of study: Study was conducted at Division of Food Science and Postharvest Technology, Indian Agricultural Research Institute, New Delhi during 2020 to 2021.

Methodology: Rice were kept for accelerated aging at 42.6°C temperature & 71% RH for a duration of 30 days. Changes in four physicochemical properties namely amylose content, volume expansion ratio (VER), water absorption ratio (WAR), and kernel elongation ratio (KER) were evaluated destructively (by spectrophotometer and cooking method) and non-destructively (by spectroradiometer) at every alternate day, during 30 days storage.

Results: The physicochemical parameters of rice showed a good correlation with spectral signatures. Subsequently, Principal component Analysis (PCA), Partial Least Square Regression (PLSR), and Multiple Linear Regression (MLR) were used to model the physicochemical changes occurring during the process of accelerated aging using spectral reflectance values. Based on values of Coefficient of determination (R^2) and Root mean square error (RMSE) accuracy of models was determined. Predictions with the MLR model resulted in a coefficient of determination (R^2) of 0.82, 0.87, 0.9, 0.83 and 0.82 with root mean square error (RMSE) of 0.18, 0.13, 0.21, 0.124 and 4.2 for amylose content, VER, WAR, KER, and ageing process respectively for calibration.

Conclusion: The study demonstrated the potential of NIRS in non-destructively predicting the physicochemical parameters of rice.

Keywords: Accelerated Ageing; Basmati rice; Non-destructive; Reflectance; Robust; Spectroradiometer.

Abbreviations:

| | |
|------|---------------------------------|
| MLR | Multiple Linear Regression |
| PLSR | Partial Least Square Regression |
| WAR | Water Absorption Ratio |
| VAR | Volume Expansion Ratio |
| KER | Kernel Elongation Ratio |
| PB | Pusa Basmati |
| PCA | Principal Component Analysis |

1. INTRODUCTION

Rice (*Oryza sativa* L.) is a global staple food, especially in South Asia, with India as a major producer after China. It is primarily grown during the kharif season (June to September) but produced year-round in select regions. Rice consumption is significant in Arabian and South Asian countries, comprising carbohydrates, starch, and various nutrients. Basmati, a fragrant rice variety, is crucial in India, leading in production and export, serving as a significant crop for the country's economy (Kaur & Chand, 2011).

35 Rice undergoes beneficial aging after harvesting, resulting in changes in physicochemical properties.
36 Aging criteria are established based on physical and chemical properties, but the exact mechanism
37 remains partly understood. Natural aging involves storing rice at room temperature for 3-6 months, a
38 time-consuming process. Accelerated aging, where rice is stored at elevated temperatures for
39 minutes to days, offers a more efficient alternative. Temperature, humidity, and storage duration are
40 key factors impacting rice quality during aging (Hussain et al., 2021).

41 Aged rice is preferred by Indian and Arabian consumers for its improved texture and premium
42 qualities, especially in the case of basmati rice known for its aroma, long grains, and excellent
43 cooking properties. Accurate assessment of rice aging is crucial to maintain quality and prevent
44 fraudulent practices. Traditional methods for assessing rice aging are complex, time-consuming, and
45 labor-intensive, requiring expensive equipment. Modern food industries demand quick, portable, and
46 non-destructive techniques for quality determination (El-Mesery et al., 2019).

47 Visible near-infrared (VNIR) spectroscopy is a valuable non-destructive technique widely used across
48 industries like agriculture, cosmetics, food, polymers, pharmaceuticals, and textiles due to its speed,
49 cost-efficiency, and minimal labor requirements (Yang et al., 2005). VNIR spectroscopy can assess
50 commodity quality in the field and during processing, relying on the scattering and absorption of light.
51 Scattering reflects external properties like particle size and density, while absorption reveals the
52 chemical composition (Birth et al., 1985).

53 VNIR spectroscopy is most successfully used for variety discrimination, determination of moisture
54 content, pH, acidity, Various sugars, various diseases/rots, and evaluation of internal quality (Qin &
55 Lu, 2007). VNIR spectroscopy works in the wavelength range between 350- 2500 nm. VNIR
56 spectrometer takes signature in terms of reflectance, absorbance, and transmittance (Jha & Garg,
57 2010). VNIR spectroscopy is used for non-destructive evaluation of rice i.e amylose content of milled
58 rice (Villareal et al., 1994; Delwiche et al., 1995), quality of rice starch (Bao et al., 2001), textural
59 properties of rice (Windham et al., 1997), quality characteristics of rice (Delwiche et al., 1996),
60 evaluation of rice wine in terms of soluble solid and pH (Liu et al., 2007).

61 This experiment utilized VNIR spectroscopy in reflectance mode to assess the aging of various
62 basmati rice varieties. The spectroradiometer's advantages include easy monitoring of the aging
63 process and improved rice grading based on age, potentially increasing market value. The study aims
64 to non-destructively analyze rice age using a VNIR spectroradiometer, with objectives to characterize
65 artificially aged rice grains through spectroscopy and physical parameters and to develop models for
66 discriminating and estimating aging in different rice grains.

67 **2. MATERIAL AND METHODS**

68 **2.1. Procurement of paddy**

69 Freshly harvested four varieties of basmati rice [Pusa Basmati (PB)- 1121, PB-1509, PB- 1637, PB-
70 1718] and one non-basmati variety [*Pusa Sugandh* (PS)] were procured from Seed Production Unit,
71 ICAR- Indian Agricultural Research Institute, New Delhi. Which was grown in the *kharif* season (June
72 to October).

73 **2.2. Sample preparation**

74 All five varieties of paddy namely PB- 1121, PB-1509, PB- 1637, PB- 1718, and PS were hulled in
75 Satake rice huller (Satake Japan). After hulling brown is rice fed to a Satake rice polisher for polishing
76 up to 6%. Broken were separated and only head rice was used for further work.

77 **2.3. Accelerated ageing of rice**

78 For accelerated ageing freshly harvested milled rice of varieties PB 1121, PB 1509, PB 1718, PB
79 1637, and Pusa Sugandh were kept in a controlled chamber maintained at Relative humidity (RH) of
80 71 %, Temperature of 42.6 ° C for a period of 30 days as suggested by Rayguru et. al. (2011) at
81 National Phytotron Facility, IARI New Delhi.

82 **2.4. Visible Near-infrared spectroscopy analysis**

83 Spectral signatures of fresh and accelerated aged samples (kept in a petri dish up to 1 cm thickness)
84 were acquired before the destructive analysis in the wavelength range between 350- 2500 nm at 1 nm

85 intervals using a handheld spectroradiometer [Analytical Spectral Device (ASD) Fieldspec®
86 Spectroradiometer (350 to 2500 nm), Boulder, USA] at Hyperspectral Remote Sensing Laboratory,
87 IARI, New Delhi. Care was taken to calibrate the device with a standard white plate before acquiring
88 the spectral signatures. The precaution was also taken to ensure no gaps between grains to avoid
89 signal losses. For each variety and accelerated storage period, six spectra were acquired to ensure
90 the repeatability of the spectral signatures. A device was calibrated after every six spectra.

91 **2.5. Determination of physicochemical properties of rice**

92 **2.5.1. Amylose content**

93 Amylose content in fresh and accelerated aged rice was determined using the spectrophotometric
94 method suggested by Juliano (1971). 100 mg rice grains were grounded using mortar and pestle and
95 transferred into the 100 ml volumetric flask. To it, 1 ml of ethanol and 10 ml of NaOH were added. The
96 mixture was heated in a boiling water bath for 10 min. Distilled water was subsequently added to
97 make the volume up to 100 ml. Out of 100 ml only 2.5 ml of the solution was then transferred into the
98 100 ml flask and 20 ml distilled water was added to it along with 3-4 drops of phenolphthalein
99 indicator till it turns pink. Then 0.1 N HCl was added drop by drop until the pink color disappears. At
100 last, 1 ml of iodine was added to it and the volume was made up to 50 ml using distilled water. The
101 absorbance of the solution was measured at 510 nm and the amylose content was determined using
102 a standard curve.

103 **2.5.2. Volume expansion ratio**

104 Volume expansion ratio (VER) was measured by using the toluene displacement method (Sidhu et
105 al., 1975). A specific volume of toluene was added to 250 ml of measuring cylinder then put 10 grains
106 of uncooked rice and the initial reading was noted. Similarly, a change in the volume of 10 grains after
107 cooking was also recorded.

$$108 \text{ VER} = \frac{V_c}{V_{uc}}$$

109 Where,

110 V_c = Volume cooked rice

111 V_{uc} = Volume of uncooked rice

112 **2.5.3. Water absorption ratio**

113 Take 10 g of milled head rice and put it into 30 g of distilled water. Then beaker was kept in a boiling
114 water bath (97 ± 2 °C) for cooking. After cooking take the final weight of the rice (Nayak &
115 Mohapatra, 2019).

$$116 \text{ WAR} = \frac{W_c - W_{uc}}{W_{uc}}$$

117 Where,

118 W_c = Weight of cooked rice

119 W_{uc} = Weight of uncooked rice

120 **2.5.4. Kernel elongation ratio**

121 It is the ratio of the average length of grain after cooking to them before cooking. 10 grains of head
122 rice were randomly selected from the sample and measured the length using a micrometer. Then
123 grains were kept for cooking and measured for the final length (Azeez and Shafi, 1966).

$$124 \text{ KER} = \frac{X_c}{X_{uc}}$$

125 Where,

126 X_c = Length of cooked rice

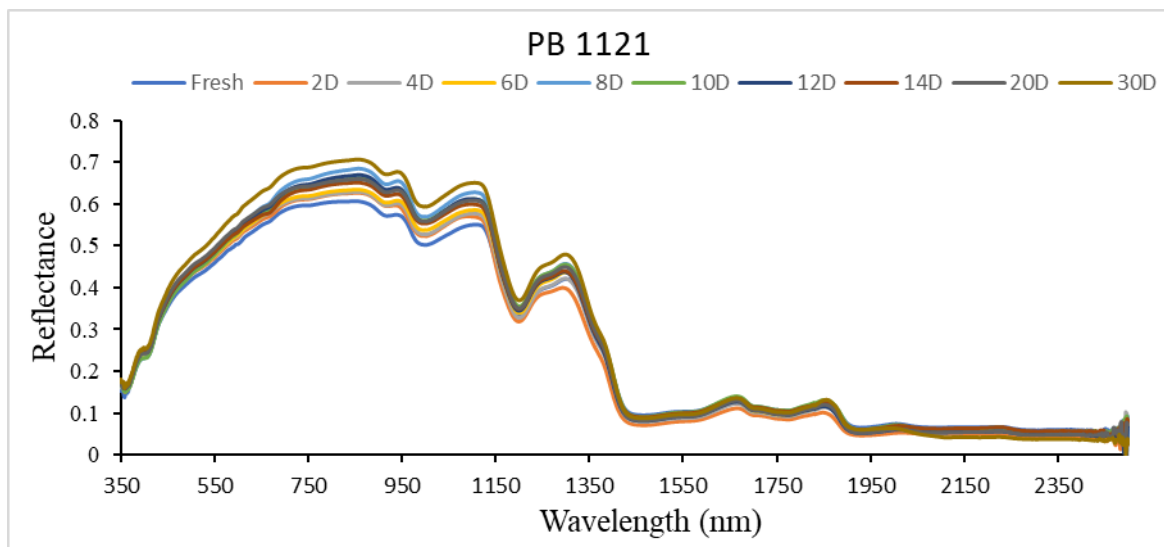
127 Xuc= Length of uncooked rice

128 2.6. Chemometric analysis and selection of wavelength

129 For performing chemometric analysis different mathematical calculations and statistical methods were
130 used. In chemometric analysis operations such as correlation, regression, calculation of the first
131 derivative, differentiation of wavelength, development of model, and evaluation of model were done
132 as described in the research work of various researchers (Nordey et al., 2017).

133 The data available after the chemometrics was too large. The next step is to reduce the huge data in
134 a particular manner and process only into selected data. Visible near-infrared (VNIR) spectroscopy
135 wavelength ranges from 350 to 2500 nm were used in this study. The Visible Near-infrared
136 reflectance spectra of rice samples shown in **Fig. 1**. In this huge range of wavelengths for each
137 parameter, it is essential to select particular ranges of wavelengths because there are close
138 relationships that can occur between wavelength and parameters. For the selection of wavelengths,
139 correlation of physicochemical parameters namely amylose content, volume expansion ratio, water
140 absorption ratio, and kernel elongation ratio with raw spectra as well as with the first derivative of
141 reflectance were performed. These correlations were done by correlating four parameters with
142 spectral reflectance data ranging from (351 to 2500 nm). As the correlation value ranges between -1
143 to 1, wavelengths showing high values of correlation were used for further analysis.

144



145

146 Fig. 1. Spectral signature of Pusa Basmati 1121 (PB 1121) after different periods of accelerated
147 storage

148 2.7. Multivariate analysis

149 Multivariate analysis of the data was conducted to develop robust models for predicting the
150 physicochemical parameters at different levels of accelerated aging and to predict the level of
151 accelerated aging of rice. Spectral reflectance values acquired at all identified promising wavelengths
152 were subjected to different available multivariate analyses like Partial least square regression (PLSR),
153 principal component analysis (PCA), and multiple linear regression (MLR). Of the data used for
154 multivariate analysis, 70% were utilized for model calibration, and the rest 30% for model validation.
155 Maximum R^2 and minimum RMSE were considered for model selection.

156 3. RESULTS AND DISCUSSION

157 3.1. Amylose content

158 The initial amylose content of rice varieties varied, with Pusa Sugandh at 22.21%, and among
159 basmati types, PB 1718 had the highest at 23.19%, followed by PB 1509 (23.12%), PB 1121
160 (22.79%), and PB 1637 (22.60%). During 30 days of accelerated storage at 42.6°C, all varieties
161 showed an increase in amylose content, with PB 1509 having the least change. This increase was

162 most significant during the first 14 days, equivalent to 7 months of ambient storage. The elevated
163 temperature likely caused amylopectin to convert into amylose, as observed in previous studies
164 (Zhong et al., 2020).

165 Amylose content significantly influences rice cooking quality. Higher amylose levels in aged rice
166 improve cooking quality and processing efficiency by reducing stickiness and increasing grain
167 firmness (Thanathornvarakul et al., 2016). This is due to lower leaching of solids during cooking (Li et
168 al., 2017) and its positive correlation with water absorption, volume expansion, fluffiness, and grain
169 separation. In the presence of lipids, amylose acts as both a diluent and a swelling inhibitor (Zhou et
170 al., 2002).

171 3.2. Volume expansion ratio (VER)

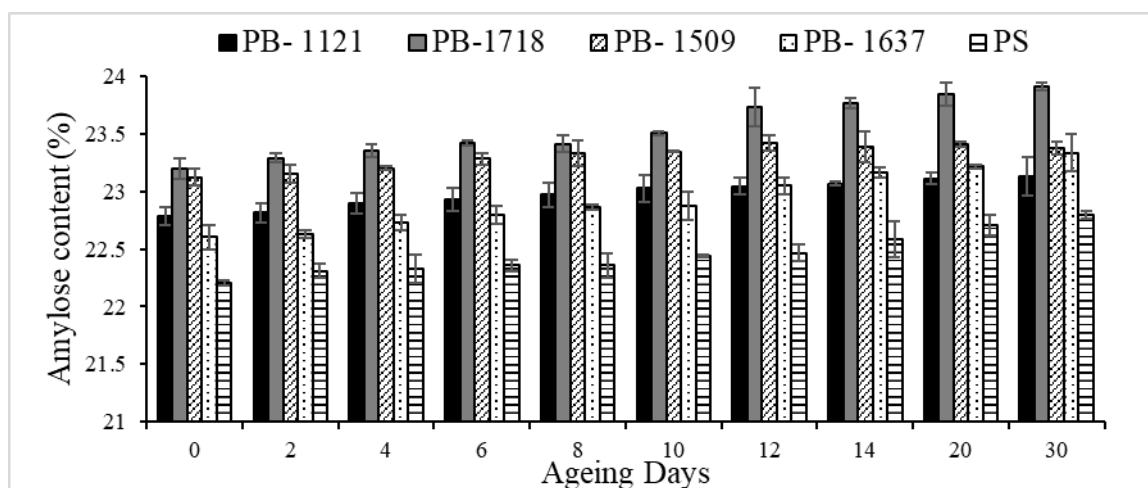
172 Volume expansion ratio (VER) is crucial for rice cooking quality. During accelerated storage, all
173 varieties showed increased VER. Pusa Sugandh had the lowest initial VER at 3.15, while basmati
174 varieties ranged from 3.51 to 3.77. After 30 days, VER increased the most for PB 1509 (4.69),
175 followed by PB 1718 (4.65), PB 1637 (4.46), PB 1121 (4.41), and Pusa Sugandh (4.20). This trend
176 aligns with previous findings regarding rice aging and amylopectin content reduction, affecting pasting
177 properties and increasing VER (Thanathornvarakul et al., 2016).

178 Accelerated storage induces structural changes in amylose chains, resulting in harder grains and
179 higher Volume Expansion Ratio (VER). Consequently, cooked rice becomes firmer and less sticky
180 due to increased water absorption and VER. Study by Indiarto & Nurannisa (2021) also support the
181 observed increase in VER during rice aging.

182 3.3. Water Absorption Ratio (WAR)

183 Water Absorption Ratio (WAR), an important cooking characteristic, mirrored the VER trend, as both
184 are positively correlated due to increased water absorption contributing to higher volume expansion
185 during cooking. Initial WAR values varied: PB 1121 (3.44), PB 1509 (3.33), PB 1637 (3.39), PB 1718
186 (3.52), and Pusa Sugandh (3.33). After 30 days of accelerated storage, WAR increased for all
187 varieties, with PB 1121 at 3.75, PB 1509 at 3.67, PB 1637 at 3.66, PB 1718 at 3.75, and Pusa
188 Sugandh at 3.59. Pusa Sugandh exhibited the least increase. Similar trends were reported by Zhou et
189 al. (2015) where aging led to increased water absorption due to rice hardness and amylose-lipid
190 complex formation.

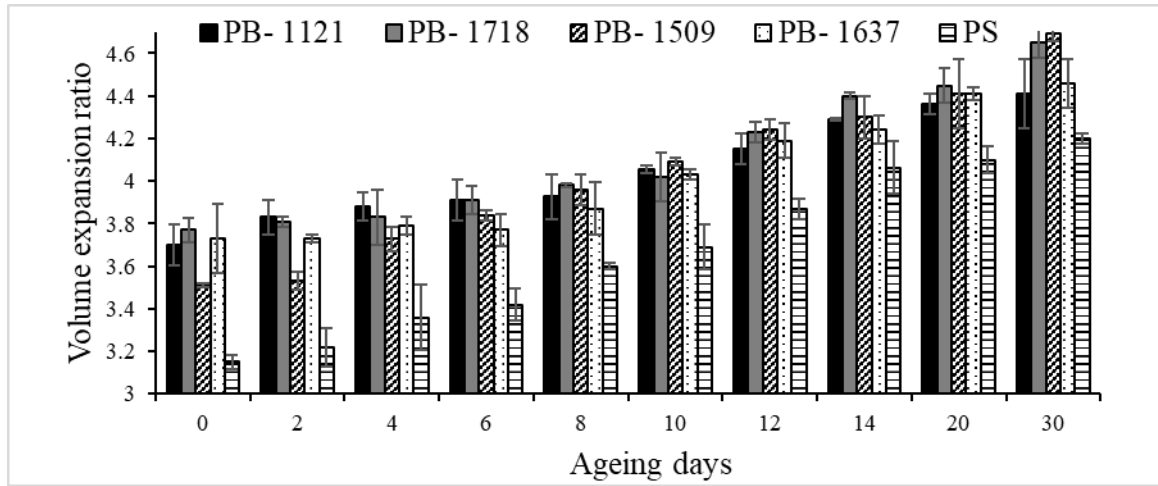
191



192

193

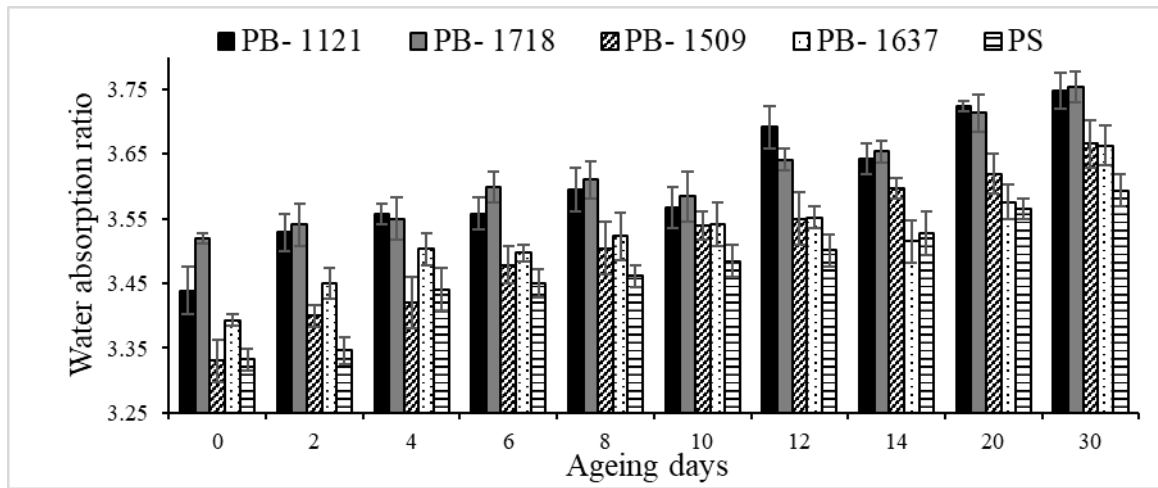
(a)



194

195

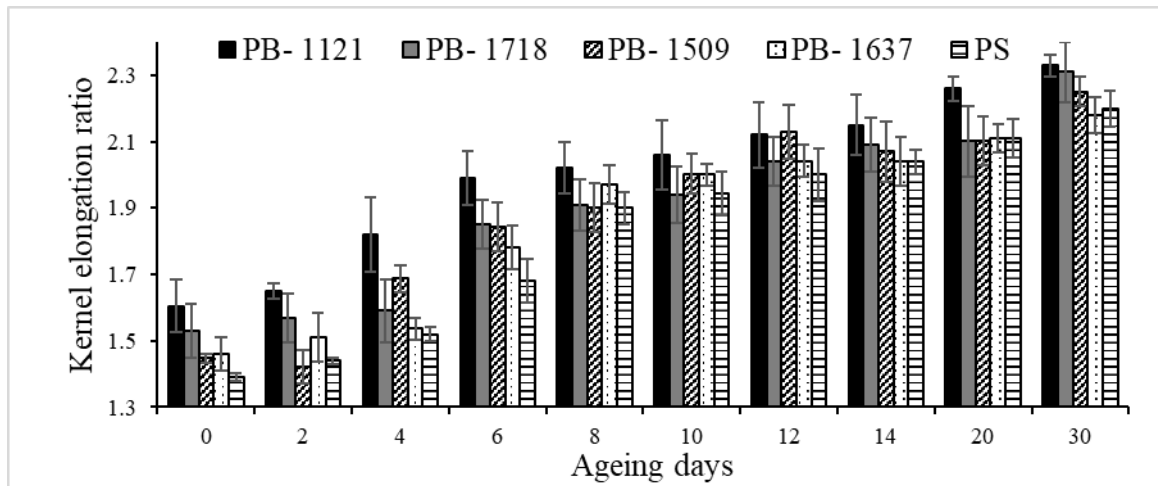
(b)



196

197

(c)



198

199

(d)

200

Fig. 2 Physicochemical changes in rice during ageing a) amylose content, b) VER, c) WAR, d) KER

201

3.4. Kernel elongation ratio (KER)

Kernel Elongation Ratio (KER) is vital for understanding rice cooking and eating quality. PB 1121 had the highest KER at 1.62, significantly surpassing all other varieties, while Pusa Sugandh had the lowest at 1.39. Among basmati types, PB 1509, PB 1637, and PB 1718 had KER values of 1.45, 1.46, and 1.49, respectively. KER generally increased during 30 days of accelerated storage, reaching 2.32 (PB 1121), 2.25 (PB 1509), 2.17 (PB 1637), 2.31 (PB 1718), and 2.20 (Pusa Sugandh) on the 30th day. The aging effect on KER followed this order: Pusa Sugandh (58.27%), PB 1509 (55.17%), PB 1718 (55.03%), PB 1637 (48.63%), and PB 1121 (43.21%). These results align with findings from Indiaro & Nurannisa (2021).

Variability in elongation ratio is linked to amylose content, particularly in PB 1121 and PB 1509, possibly due to amylose structure and its interaction with protein and lipids during accelerated storage. Starch granule expansion without disintegration depends on amylose content (Juliano, 1985), aligning with VER and WAR trends governed by structural changes and amylose content. Aging efficiency varies with rice variety, pre-treatments, techniques, and storage conditions (Indiaro & Nurannisa, 2021).

3.5 Multivariate analysis and modeling

Spectral signatures were correlated with physicochemical parameters and aging duration, yielding correlation coefficients from -0.1 to 0.85 in the 400-1500 nm wavelength range. Correlation of raw spectral signatures with physicochemical parameters spanned wide wavelength ranges, making wavelength selection challenging. To address this, mathematical transformations, specifically 1st derivatives of spectral reflectance values, were employed. Correlation analysis revealed wavelength bands of interest: 1500-1800 nm for amylose content, 1200-1800 nm for VER, 1100-1800 nm for WAR, 500-1300 nm for KER, and 950-1400 nm for accelerated aging duration. For KER, correlation coefficients surpassed ± 0.8 at 1150-1350 nm. The derivatives demonstrated higher maximum correlation coefficients compared to raw spectral reflectance values (Table 1).

Table 1 Wavelengths showing maximum correlation with first derivative spectral reflectance

| Parameter | Max. correlation | Wavelength range (nm) |
|-----------------|------------------|-----------------------|
| Amylose content | 0.7917 | 1500-1800 |
| VER | 0.7982 | 1200-1800 |
| WAR | 0.7630 | 1100-1800 |
| KER | 0.8463 | 500-1300 |

3.5.1 Amylose content

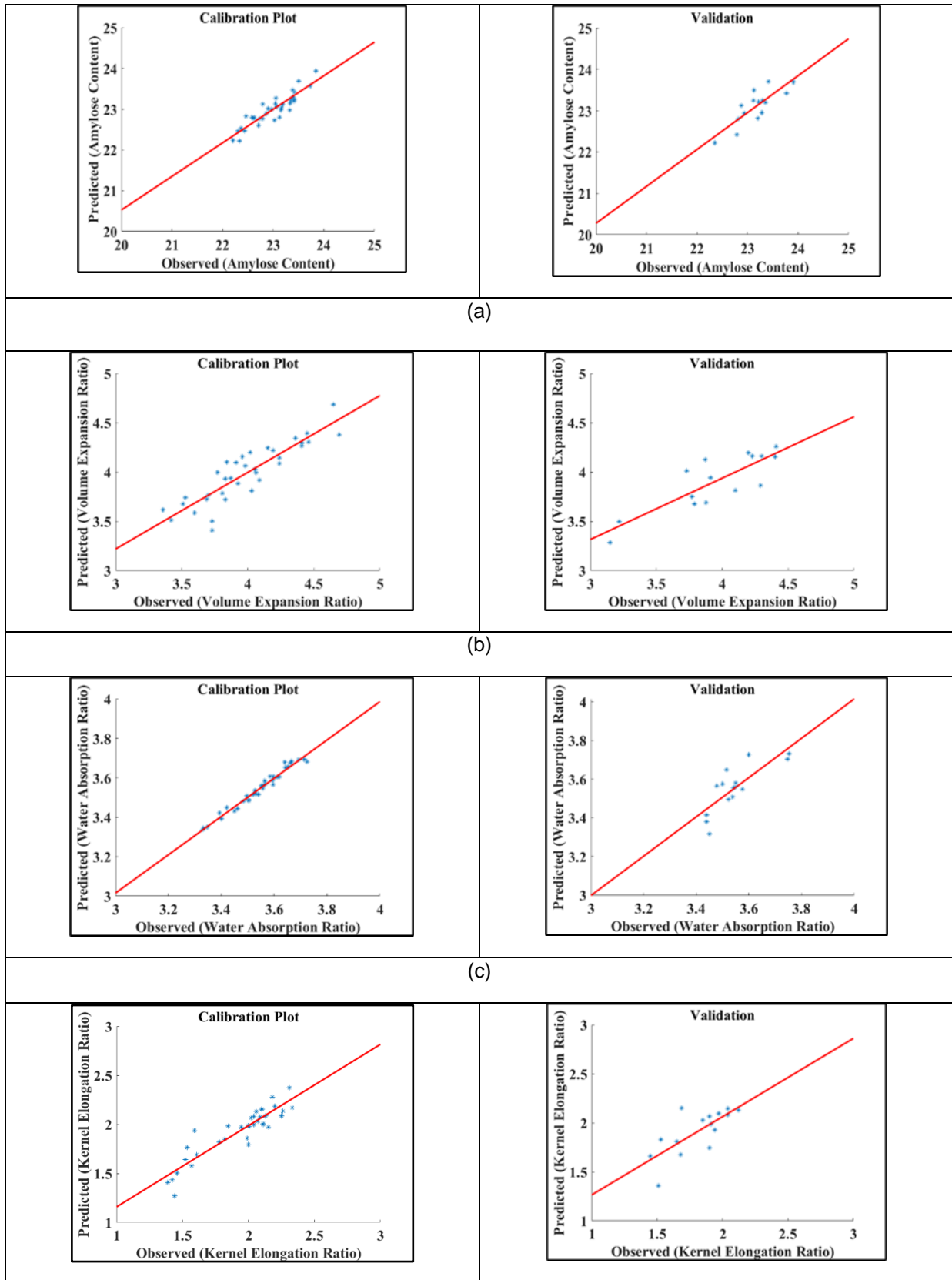
Amylose content changes during rice accelerated aging, affecting grain texture and cooking properties. PLSR models were developed using data in the 1500-1800 nm wavelength range, resulting in R^2 values of 0.65 (calibration) and 0.90 (validation), with an RMSE of 0.23. PCA showed that the first three principal components explained 94% of the variability. Subsequently, MLR modeling using sensitive wavelengths in the 1500-1800 nm range yielded R^2 values of 0.82 (calibration) and 0.84 (validation) with RMSE values of 0.186 and 0.210, respectively (Fig. 3a).

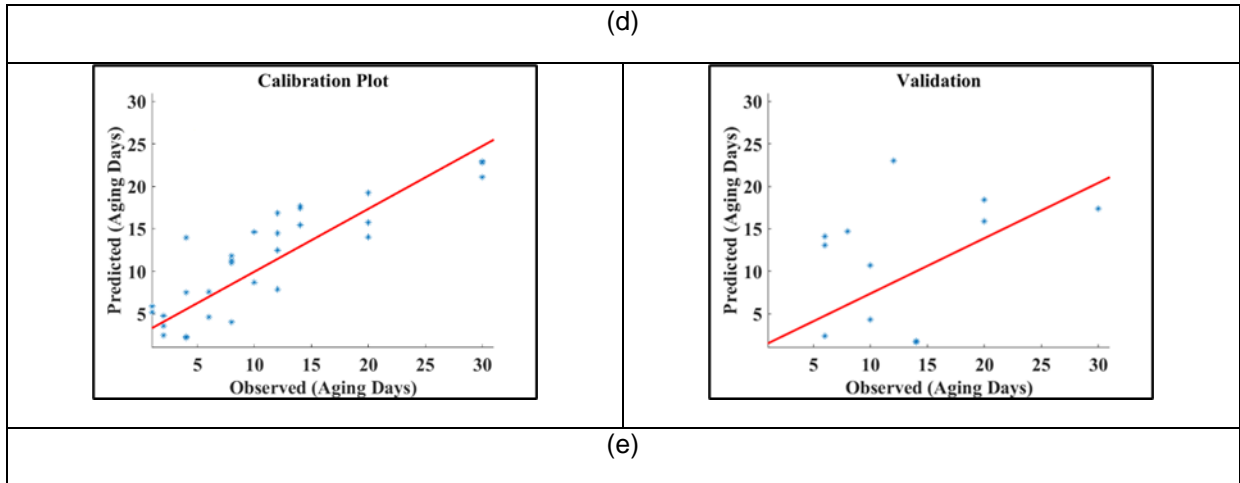
Matsuo et al. (2018) employed NIR spectroscopy, achieving an R^2 of 0.72 for amylose content in Japonica rice within the 850-1048 nm range. Fernández-Novales et al. (2009) determined reducing sugars in grape ripening using Shortwave-NIR spectroscopy, obtaining an R^2 of 0.92 (800-1050 nm). Bao et al. (2001) predicted rice starch quality with a spectroradiometer, yielding an R^2 of approximately 0.91 for amylose content (400-2500 nm). He et al. (2021) used NIR spectroscopy for cereals, attaining R^2 values above 0.9 in the 1923-1961 nm range for starch and amylose content.

3.5.2 Volume Expansion Ratio

Similar to the amylose content approach, VER was correlated with spectral signatures. The first three principal components explained 94.6% of VER variability, with loading values peaking between 1200-1800 nm. PLSR models had R^2 values of 0.50 (calibration) and 0.67 (validation), with RMSE of 0.21. MLR models yielded R^2 values of 0.87 (calibration) and 0.85 (validation), with RMSE values of 0.13 and 0.15, respectively (Fig. 3b).

247 Moghimi et al., (2010) attempted to develop calibration models for evaluating the TSS and acidity of
 248 kiwifruit. They developed a model using principal component analysis (PCA) and partial least square
 249 regression (PLS). The correlation coefficients for TSS and acidity were 0.93 and 0.943 respectively.
 250 RMSE values were 0.076% and 0.26°Brix respectively obtained between wavelength region of 400 to
 251 1000 nm.





252 Fig. 3 MLR models for prediction of a) amylose content, b) VER, c) WAR, d) KER, e) ageing

253 **3.5.3 Water expansion ratio**

254 For water expansion ratio, the first three principal components explained 93.6% of the variability, with
 255 loading values peaking at 1100-1800 nm. PLSR models achieved R^2 values of 0.78 (calibration) and
 256 0.70 (validation), with RMSE of 0.044. MLR models obtained R^2 values of 0.97 (calibration) and 0.90
 257 (validation), with RMSE values of 0.21 and 0.25, respectively (Fig. 3c). In a study by Kusumiyati et al.
 258 (2021) on apple fruit quality evaluation, NIR spectroradiometer yielded an R^2 of 0.81 and RMSE of
 259 0.009 for water content within the 702-1065 nm wavelength band.

260 **3.5.4 Kernel elongation ratio**

261 For kernel elongation ratio (KER), the first three principal components explained 96% of the variability,
 262 with loading values peaking at 500-1300 nm wavelengths. PLSR models achieved R^2 values of 0.64
 263 (calibration) and 0.84 (validation), with RMSE of 0.16 and 0.15. MLR models obtained R^2 values of
 264 0.83 (calibration) and 0.85 (validation), with RMSE values of 0.124 and 0.11, respectively (Fig. 3d). In
 265 a study by Schmilovitch et al. (2000) on mango physiological indices using NIR spectroscopy, MLR
 266 models had R^2 values of 0.92 for TSS and 0.6085 for acidity in the 1200-2400 nm wavelength region,
 267 outperforming PLSR models.

268 **3.5.5 Ageing of rice**

269 For accelerated aging, spectral signatures were correlated similarly to amylose content. The first three
 270 principal components explained 96% of the variability. PLSR models achieved R^2 values of 0.42
 271 (calibration) and 0.58 (validation), with RMSE of 6.27. MLR models obtained R^2 values of 0.82
 272 (calibration) and 0.70 (validation), with RMSE values of 4.2 and 4.5, respectively (Figure 3e). In a
 273 study by Fernández-Navales et al. (2009) on wine quality prediction during aging using NIR
 274 spectroscopy, it was found to be a promising technique for assessing grape wine quality attributes
 275 during fermentation and aging.

276 The chemometric analysis indicated that spectral reflectance values between 350 to 2500 nm could
 277 adequately predict quality. MLR outperformed PLSR in terms of R^2 and RMSE in both calibration and
 278 validation. MLR's superior performance is attributed to its selective wavelength choice, eliminating
 279 overfitting and collinearity issues observed in PLSR models (Table 2) (EIMasry et al., 2007;
 280 Fernández-Navales et al., 2009).

281 **Table 2** Summary of PLSR and MLR statistics for Amylose content, VER, WAR, KER, and Ageing

| Parameters | MLR Model | | | | PLSR Model | | | |
|------------------------|-------------|------|------------|------|-------------|------|------------|------|
| | Calibration | | Validation | | Calibration | | Validation | |
| | R^2 | RMSE | R^2 | RMSE | R^2 | RMSE | R^2 | RMSE |
| Amylose content | 0.82 | 0.18 | 0.84 | 0.21 | 0.64 | 0.23 | 0.90 | 0.23 |

| | | | | | | | | |
|---------------|------|-------|------|------|------|------|------|------|
| VER | 0.87 | 0.13 | 0.85 | 0.15 | 0.50 | 0.21 | 0.67 | 0.21 |
| WAR | 0.97 | 0.21 | 0.90 | 0.25 | 0.77 | 0.04 | 0.70 | 0.04 |
| KER | 0.83 | 0.124 | 0.85 | 0.11 | 0.63 | 0.15 | 0.84 | 0.15 |
| Ageing | 0.82 | 4.2 | 0.70 | 4.5 | 0.42 | 6.27 | 0.57 | 6.27 |

282

283 **4 CONCLUSION**

284 Physicochemical changes during accelerated rice aging were assessed both destructively and non-
285 destructively. Spectral reflectance, including first derivatives, correlated with these changes and aging
286 periods. PCA, PLSR, and MLR were used to develop predictive models.

- 287 • Spectral reflectance effectively captures amylose content, VER, WAR, and KER changes
288 during rice aging, enabling age determination.
- 289 • Variabilities in physical parameters and aging were characterized within 600-1800 nm using
290 raw spectral reflectance, and 900-1350 nm using 1st derivatives.
- 291 • MLR models outperformed PLSR models, achieving $R^2 > 0.80$ for physical parameters and
292 age prediction (PLSR R^2 : 0.42-0.77).

293 **CRedit authorship contribution statement**

294 Patil Rajvardhan Kiran: Experimental analysis, Collecting dataset, Investigation, Original draft
295 preparation. Abhijit Kar: Conceptualization, Methodology. Rabi Narayan Sahoo: Conceptualization,
296 Methodology. Arunkumar T. V.: Investigation, Review and editing.

297 **Declaration of competing interest**

298 The authors declare that they have no known competing financial interests or personal relationships
299 that could have appeared to influence the work reported in this paper.

300 **Acknowledgement**

301 We acknowledge the support extended by staff of Indian Agricultural Research Institute (IARI), New
302 Delhi and Indian Council of Agricultural Research, New Delhi for financial support in the form of Junior
303 Research Fellowship.

304 **Funding Agency**

305 This research did not receive any specific grant from funding agencies in the public, commercial nor-
306 for-profit sectors.

307 This research did not receive any specific grant from funding agencies in the public, commercial nor-
308 for-profit sectors.

309 **References**

310 Azeez MA, Shafi M, Quality in Rice. Department of Agriculture, West Pakistan Technology. 1966;
311 Bulletin. No. 13: 50.

312 Bao JS, Cai, YZ, Corke H, Prediction of Rice Starch Quality Parameters by Near-Infrared Reflectance
313 Spectroscopy. J. Food Sci. 2001, 66(7): 936–939. <https://doi.org/10.1111/j.1365-2621.2001.tb08215.x>

314 Birth G S, Dull GG, Renfroe WT, Kays SJ, Nondestructive Spectrophotometric Determination of Dry
315 Matter in Onions. J Am. Soc. Hortic. Sci. 1985, 110(2): 297–303.
316 <https://doi.org/10.21273/JASHS.110.2.297>

317 Delwiche SR, Bean MM, Miller RE, Webb BD, Williams PC, Apparent amylose content of milled rice
318 by near-infrared reflectance spectrophotometry. 1995

- 319 Delwiche SR, McKENZIE KS, Webb BD, Quality characteristics in rice by near-infrared reflectance
320 analysis of whole-grain milled samples. 1996
- 321 ElMasry G, Wang N, ElSayed A, Ngadi M, Hyperspectral imaging for nondestructive determination of
322 some quality attributes for strawberry. *J. Food Eng.* 2017, 81(1): 98–107.
323 <https://doi.org/10.1016/j.jfoodeng.2006.10.016>
- 324 El-Mesery H, Mao H, Abomohra A, Applications of Non-destructive Technologies for Agricultural and
325 Food Products Quality Inspection. *Sensors* 2019, 19(4): 846. <https://doi.org/10.3390/s19040846>
- 326 Fernández-Navales J, López MI, Sánchez MT, Morales J, González-Caballero V, Shortwave-near
327 infrared spectroscopy for determination of reducing sugar content during grape ripening, winemaking,
328 and aging of white and red wines. *Food Res. Int.* 2009, 2(2): 285–291.
329 <https://doi.org/10.1016/j.foodres.2008.11.008>
- 330 He, M, Hu J, Wu Y, Ouyang J, Determination of starch and amylose contents in various cereals using
331 common model of near-infrared reflectance spectroscopy. *Int. Food Res. J.* 2021, 28(5): 987–995.
332 <https://doi.org/10.47836/ifrj.28.5.12>
- 333 Hussain, S. Z., Iftikhar, F., Naseer, B., Altaf, U., Reshi, M., & Nidoni, U. K., 2021. Effect of
334 radiofrequency induced accelerated ageing on physico-chemical, cooking, pasting and textural
335 properties of rice. *LWT* 139: 110595. <https://doi.org/10.1016/j.lwt.2020.110595>
- 336 Indiarito, R., & Nurannisa, R. L., 2021. Aging Technique Of Rice And Its Characteristics. 10(01).
- 337 Jha SN, Garg R, Non-destructive prediction of quality of intact apple using near infrared spectroscopy.
338 *J. Food Sci. Technol.* 2010, 47(2): 207–213.
- 339 Juliano, B. O. Factors affecting nutritional properties of rice protein. *Trans Natl Acad Sci Technol.*
340 1985; 7: 205-216.
- 341 Kaur J, Chand T, Effect of Natural Ageing of Basmati Paddy on Physico-chemical and Textural
342 Properties of Cooked Rice. *J. Agric. Eng.* 2011, 48(2): 1–6.
- 343 Kusumiyati K, Hadiwijaya Y, Suhandy D, Munawar AA, Prediction of water content and soluble solids
344 content of 'manalagi' apples using near infrared spectroscopy. *IOP Conference Series: Earth and*
345 *Environmental Science* 2021, 922(1): 012062. <https://doi.org/10.1088/1755-1315/922/1/012062>
- 346 Li H, Fitzgerald MA, Prakash S, Nicholson TM, Gilbert R G, The molecular structural features
347 controlling stickiness in cooked rice, a major palatability determinant. *Sci. Rep.* 2017, 7(1): 1–12.
- 348 Liu F, He Y, Wang L, Pan H, Feasibility of the use of visible and near infrared spectroscopy to assess
349 soluble solids content and pH of rice wines. *J Food Eng.* 2007, 83(3): 430–435.
350 <https://doi.org/10.1016/j.jfoodeng.2007.03.035>
- 351 Matsuo, M., Kawamura, S., Kato, M., Diaz, E. O., & Koseki, S. Practical Application of Near-Infrared
352 Spectroscopy for Determining Rice Amylose Content at Grain Elevator. *Arid Zone Journal Of*
353 *Engineering, Technology And Environment.* 2018; 14(SP.i4): 95-100.
- 354 Moghimi A, Aghkhani MH, Sazgarnia A, Sarmad M, Vis/NIR spectroscopy and chemometrics for the
355 prediction of soluble solids content and acidity (pH) of kiwifruit. *Biosys. Eng.* 2010, 106(3): 295–302.
356 <https://doi.org/10.1016/j.biosystemseng.2010.04.002>
- 357 Nayak M, Mohapatra M, Effect of microwave heating on accelerated aging qualities of rice. *Oryza,*
358 2019, 56(2), 228–235.
- 359 Nordey T, Joas J, Davrieux F, Chillet M, Léchaudel M, Robust NIRS models for non-destructive
360 prediction of mango internal quality. *Sci. Hortic.* 2017, 216, 51–57.
361 <https://doi.org/10.1016/j.scienta.2016.12.023>
- 362 Qin J, Lu R, Measurement of the absorption and scattering properties of turbid liquid foods using
363 hyperspectral imaging. *Applied Spectroscopy* 2007, 61(4): 388–396.

- 364 Rayaguru K, Pandey JP, Routray W. Optimization of process variables for accelerated aging of
365 basmati rice. *Journal of Food Quality*. 2011 Feb;34(1):56-63.
- 366 Schmilovitch Z, Mizrach A, Hoffman A, Egozi, H, Fuchs Y, Determination of mango physiological
367 indices by near-infrared spectrometry. *Postharvest Biol. Technol.* 2000, 19(3): 245–252.
368 [https://doi.org/10.1016/S0925-5214\(00\)00102-2](https://doi.org/10.1016/S0925-5214(00)00102-2)
- 369 Sidhu JS, Gill M S, Bains GS. Milling of paddy in relation to yield and quality of rice of different Indian
370 varieties. *J. Agric. Food Chem.* 1975; 23(6): 1183-1185. <https://doi.org/10.1021/jf60202a035>
- 371 Thanathornvarakul N, Anuntagool J, Tananuwong K, Aging of low and high amylose rice at elevated
372 temperature: Mechanism and predictive modeling. *J. Cereal Sci.* 2016, 70: 155–163.
- 373 Villareal CP, De La Cruz NM, Juliano BO, Rice amylose analysis by near-infrared transmittance
374 spectroscopy. *Cereal Chem.* 1994, 71(3): 292–296.
- 375 Windham WR, Lyon BG, Champagne ET, Barton FE, Webb BD, McClung AM, Moldenhauer KA,
376 Linscombe S, McKenzie KS. Prediction of cooked rice texture quality using near-infrared reflectance
377 analysis of whole-grain milled samples. *Cereal Chem.*, 1997 Sep;74(5):626-32.
- 378 Yang CC, Chao K, Chen YR, Early HL, Systemically diseased chicken identification using
379 multispectral images and region of interest analysis. *Comput. Electron. Agric.* 2005, 49(2): 255–271.
- 380 Zhong, Y., Xiang, X., Chen, T., Zou, P., Liu, Y., Ye, J., ... & Liu, C. Accelerated aging of rice by
381 controlled microwave treatment. *Food chemistry*. 2020; 323: 126853.
- 382 Zhou Z, Robards K, Helliwell S, Blanchard C, Ageing of Stored Rice: Changes in Chemical and
383 Physical Attributes. *J Cereal Sci.* 2002, 35(1): 65–78. <https://doi.org/10.1006/jcrs.2001.0418>
- 384 Zhou Z, Wang X, Si X, Blanchard C, Strappe P, The ageing mechanism of stored rice: A concept
385 model from the past to the present. *J. Stored Prod. Res.* 2015, 4: 80–87.
386 <https://doi.org/10.1016/j.jspr.2015.09.004>